

Isomerism in Copper(I)-Induced Folding of Homoditopic Macrocyclic Ligands with Bis(dithiadiimine) Donor Sets

Peter Comba*^[a] and Andreas Kühner^[a]

Keywords: Macrocyclic ligands / Molecular modeling / Schiff bases / Helical structures / Copper

The structural properties of the dicopper(I) compounds of the two large macrocyclic Schiff base ligands *para*-222 and *meta*-222 with two dithiadiimine coordination sites, where the two sites are linked by two *para*- or two *meta*-xylylene spacer groups and all bridges between the donors of each site are ethylene groups (32- and 30-membered macrocycles for the *para*- or *meta*-xylylen-bridged *para*-222 and *meta*-222 species, respectively) are studied, in solution and by computer modeling. Solid-state structural data have been reported elsewhere. The coordination of the 32-membered macrocycle *para*-222 to two copper(I) centers leads to a helical figure-of-eight-shaped structure. Two diastereomeric pairs of enantiomers have been observed for this type of

compound in solution. The crystallized form is more stable than the second isomer by approximately 6–10 kJ/mol (solution-NMR spectroscopy and force-field calculations). Both experimentally detected isomers are more than 15 kJ/mol more stable than the other five possible configurations (force-field calculations). For the *meta*-222 macrocycle (30-membered ring) an achiral structure has been observed in the solid while two of the 21 possible isomers have been detected in solution (3:1, NMR spectroscopy). The computed structures and isomer distributions (force-field calculations) are compared with the solid-state structures and with observed isomer distributions from NMR experiments, and dynamic processes are analyzed in detail.

Introduction

The coordination of the paracyclophane-based preorganized double-helical (N₂S₂)₂ bis(dithiadiimine) ligand (phane-222, see Figure 1) to copper(I) yields a dicopper(I) complex that, based on the observed structure, is not much strained.^[1] Indeed, the coordination of copper(I) to analogous macrocyclic ligands, where the two (N₂S₂)₂ donor sites are linked by two *para*-xylylene groups (*para*-222, see Figure 1) leads to a very similar figure-of-eight-shaped structure.^[2–4] That is, copper(I) induces an identical folding, and this indicates that phane-222 is highly preorganized for copper(I).^[5–7] The isomer with *meta*-xylylene-bridged donor groups (30- instead of 32-membered macrocyclic ring, *meta*-222, see Figure 1) leads to an achiral dicopper(I) compound but the overall shape of the structure (“squeezed” instead of “twisted” figure-of-eight shape) and, in particular, the geometry of the chromophores are very similar.^[3] Plots of the observed structures of the three dicopper(I) compounds are shown in Figure 1 and relevant parameters are assembled in Table 1.

From solid-state structural studies of an extended series of dicopper(I) compounds of Schiff base (N₂S₂)₂ ligands of the general type shown in Figure 1 (variation of the aromatic spacer groups, variation of the chelate ring sizes) it emerges that, for the chiral compounds with *para*-substituted spacer groups (e.g. *para*-222), only one of seven possible diastereoisomeric pairs of enantiomers is observed, that is, one of the two forms that have identical configuration for all four coordinated thioether-S donors (see below

and Figure 1); for the *meso* form (*meta*-222) the thioether-S configurations are (R)(R)(S)(S) and only one of three theoretically possible isomers with respect to the orientation of the xylylene spacer groups is observed in the crystal structural analysis (see Figure 1).^[3,4]

Solution-NMR studies indicate that the geometries in solution are identical to those observed in the solid, that is figure-of-eight-shaped (“twisted” or “squeezed” for *para*- and *meta*-substituted xylylene spacer groups, respectively), and that dynamic processes occur. The dicopper(I) compounds of *para*-222 and of derivatives with larger chelate ring sizes have been studied in detail by solution-NMR spectroscopy.^[4] An intramolecular dynamic process leads to helix inversion (epimerization, that is, retention of the configuration of the S donors), and a solvent-dependent intermolecular process leads to full racemization.^[4] For the derivative of *para*-222 with two seven-membered chelate rings (*para*-242) there is spectroscopic evidence for an equilibrium with a less stable isomer, and this is attributed to the helix inversion (epimerization) product.^[4] The solution chemistry of *meta*-222 is addressed here. We also present a full conformational analysis of the two isomers [Cu₂(*para*-222)]²⁺ and [Cu₂(*meta*-222)]²⁺, based on force-field calculations, and these are compared to observed solid-state and solution data.

Results and Discussion

Isomerism

The helical dinuclear compounds, that is, the dicopper(I) compounds of phane-222 and *para*-222, have the same shape and the same idealized symmetry (*D*₂) while the achiral dicopper(I) compound, that is, that of *meta*-222 has ide-

^[a] Anorganisch-Chemisches Institut der Universität Heidelberg, Im Neuenheimer Feld 270, D-69120 Heidelberg, Germany
Fax: (internat.) +49(0)6221-54 66 17
E-mail: comba@akcomba.oci.uni-heidelberg.de

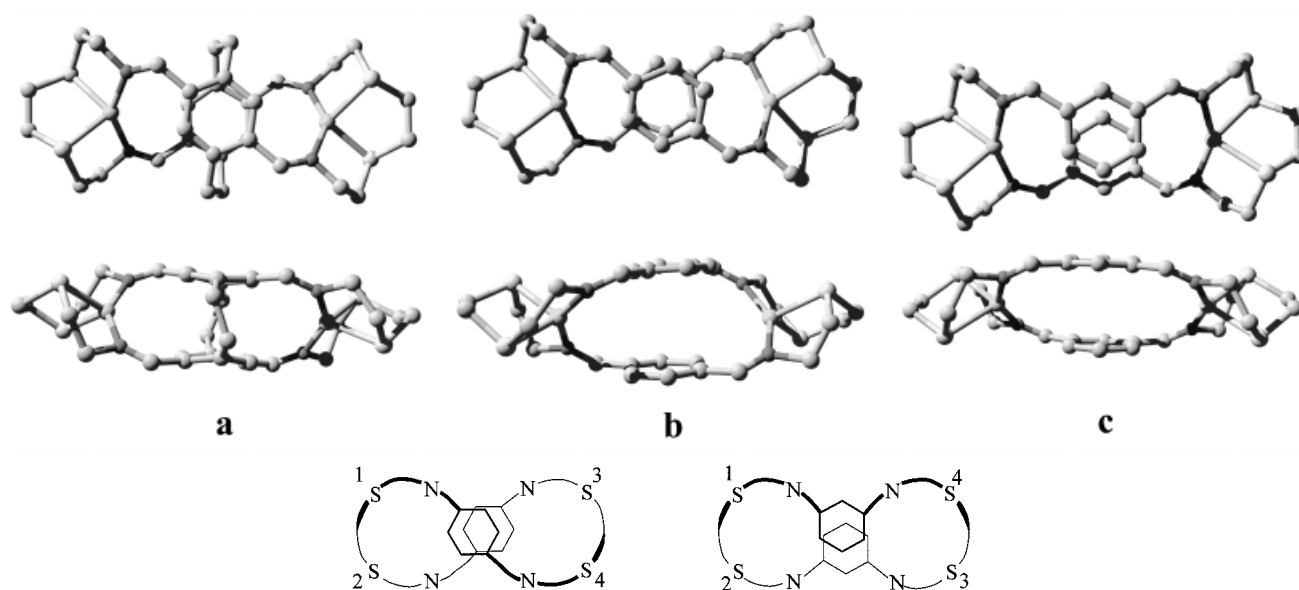


Figure 1. Plots of the molecular cations of the experimentally observed solid-state structures of (a) $[\text{Cu}_2(\text{phane-222})]^{2+}$,^[1] (b) $[\text{Cu}_2(\text{para-222})]^{2+}$,^[3] (c) $[\text{Cu}_2(\text{meta-222})]^{2+}$,^[3] and sketches of the “helical” and “squeezed” folding of the macrocycles with numbering scheme

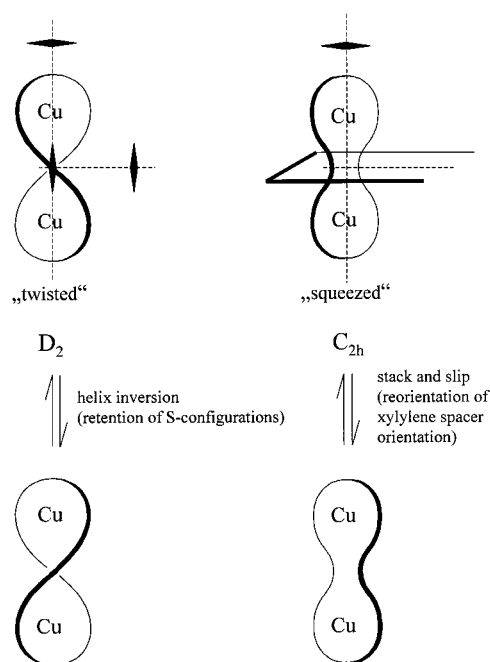
Table 1. Structural parameters of $[\text{Cu}_2(\text{phane-222})]^{2+}$,^[1] $[\text{Cu}_2(\text{para-222})]^{2+}$,^[3] and $[\text{Cu}_2(\text{meta-222})]^{2+}$,^[3]

Ligand	phane-222	para-222	meta-222
Cu–S	2.42	2.38	2.43
Cu–N	1.96	2.01	1.99
Cu···Cu	8.22	7.83	8.15
Cxyl···Cxyl	—	3.43	3.26; 3.43
xyl···xyl	3.09	3.59	3.39
S–Cu–S	91.51	91.0	88.2
S–Cu–N	117.4	115.1	113.3
S–Cu–N ^{bite}	90.2	90.8	89.7
N–Cu–N	141.2	144.1	148.5
C _{imine} –C _{xyl[a]}	32	31	27
θ ^[b]	71	73	73

[a] Torsional angle around the imine bond. — [b] Tetrahedral twist angle (S–Cu–S; N–Cu–N planes; tetrahedral: 90°).

alized C_{2h} symmetry (see Scheme 1). For $[\text{Cu}_2(\text{para-222})]^{2+}$ there are eleven elements of asymmetry, the helix, the four thioether-S donors and the six five-membered chelate rings. The experimentally determined structure has Λ -(S)(S)(S)(S)- $\lambda\lambda\lambda\lambda\lambda\lambda$ geometry (the order of the thioether-S configurations and of the five-membered chelate ring conformations is based on the numbering scheme given in Figure 1; the same conformation is observed in all other structurally determined derivatives^[4]). There are seven diastereomeric pairs of enantiomers with different sequences of thioether-S configurations [Λ -helices: (S)(S)(S)(S), (S)(S)(S)(R), (S)(S)(R)(R), (S)(R)(R)(S), (S)(R)(S)(R), (R)(R)(R)(S) and (R)(R)(R)(R)]. For each there is a number of possible sequences of the five-membered chelate ring conformations, leading to 350 non-degenerate isomers.

The $[\text{Cu}_2(\text{meta-222})]^{2+}$ ion has twelve stereochemical elements, the four thioether-S donors, the six five-membered chelate ring conformations and the orientation of the two *meta*-xylylene spacer groups. The crystallized molecule has



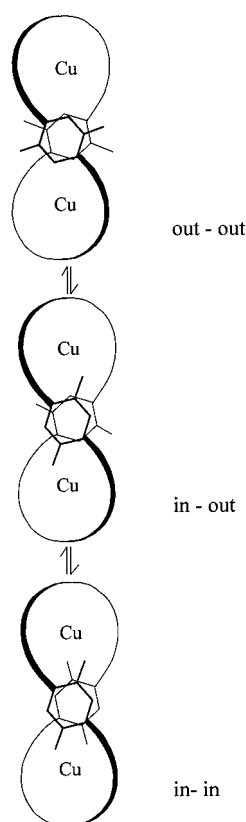
Scheme 1

tail-to-tail-(S)(S)(R)(R)- $\lambda\lambda\lambda\delta\delta\delta$ geometry (the nomenclature follows the numbering scheme given in Figure 1; tail-to-tail refers to the orientation of the *meta*-xylylene bridges, see Scheme 3, below). There are 72 non-degenerate isomers in this system.

Dynamics – Experimental Observations

High-resolution ^1H -NMR spectroscopy indicates that, for both structural types, the figure-of-eight-shaped geometry is retained in solution.^[1–4] For the helical dicop-

per(I) compounds (e.g. $[\text{Cu}_2(\text{para-222})]^{2+}$) there is evidence for two independent dynamic processes.^[4] The first is helix inversion with full retention of the thioether-S configuration (epimerization). This is observed at low temperature in solvents with little affinity to copper(I) (intramolecular reaction, observed in nitromethane) in the low-field region of the $^1\text{H-NMR}$ spectrum (non-equivalent aromatic protons, see Scheme 2).^[4] For a derivative of *para-222* (i.e. *para-242*) there is spectroscopic evidence for the second diastereoisomer that emerges from helix inversion [Δ -(*S*)(*S*)(*S*)(*S*) versus Λ -(*S*)(*S*)(*S*)(*S*)]. For *para-222* the helix inversion has a lower energy barrier and the spectra were therefore not fully resolved at the lowest temperature available in nitromethane.^[4] The comparison of the temperature-dependent $^1\text{H-NMR}$ data of the dicopper(I) compounds of *para-222* with those of ligands with substituted benzene spacer groups (e.g. *Me-para-222*, see Scheme 2, dimethylated spacer group) suggests that along the helix inversion mode there is rotation of the xylene groups around the C1...C4 axes (in/out isomerism, see Scheme 2).^[4] The rate of this rotation depends on the size of the xylene substituents.

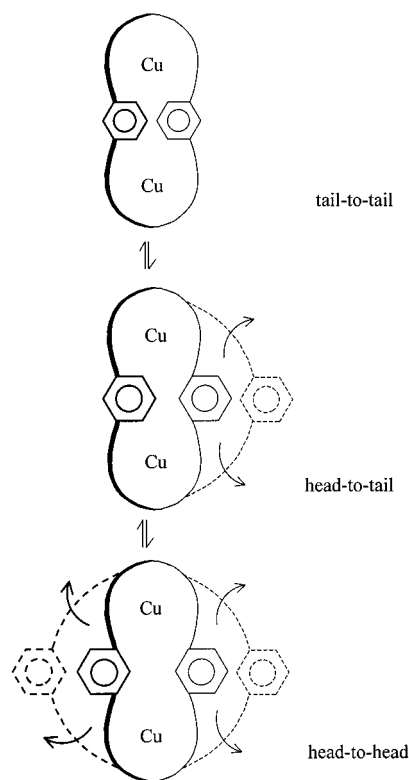


Scheme 2

The second dynamic process leads to full racemization, that is, it involves inversion of the helix *and* inversion at each of the four thioether-S donors [Λ -(*S*)(*S*)(*S*)(*S*) versus Δ -(*R*)(*R*)(*R*)(*R*)]. This reaction is only observed in acetonitrile for which copper(I) has a strong affinity. It occurs at significantly higher temperatures than the helix inversion, and it was assigned on the basis of temperature-dependent

$^1\text{H-NMR}$ spectra in the high-field region (methylene protons).^[4] The solvent dependence and the fact that inversion at the thioether-S donors involves copper(I)–S bond breaking suggest that full racemization is an intermolecular process. This was supported by crystallization and the structural analysis of a putative intermediate with two coordinated acetonitrile molecules.^[4]

The solution $^1\text{H-NMR}$ spectroscopic behavior of the achiral $[\text{Cu}_2(\text{meta-222})]^{2+}$ cation is strikingly different. In both solvents, acetonitrile and nitromethane, there are, in dependence of the temperature, two types of spectra: a well-resolved low-temperature spectrum (for the region of aromatic and imine protons, see Figure 2) and a high-temperature spectrum that has coupling patterns identical to those of the metal-free ligand but chemical shifts (methylene protons, high-field region) that indicate copper(I) coordination. In analogy to the observations and interpretations with the helical compounds^[4] (see above), the high-temperature spectrum is attributed to a species, where a dynamic process leads to full scrambling which may involve a “stack-and-slip” process (Scheme 1), reorientation of the *meta*-xylene spacer groups (Scheme 3) and inversion at the thioether-S centers.



Scheme 3

In contrast to observations with the “twisted” geometries (helical compounds, e.g. $[\text{Cu}_2(\text{para-222})]^{2+}$, see above^[4]) with the “squeezed” geometry ($[\text{Cu}_2(\text{meta-222})]^{2+}$) this process occurs in acetonitrile *and* in nitromethane $\{[\text{Cu}_2(\text{meta-222})]^{2+}$: coalescence temperatures for the aromatic protons: 330 K (nitromethane), 300 K (nitromethane/acetonitrile, 10:1), 250 K (acetonitrile); $[\text{Cu}_2(\text{para-222})]^{2+}$, aromatic pro-

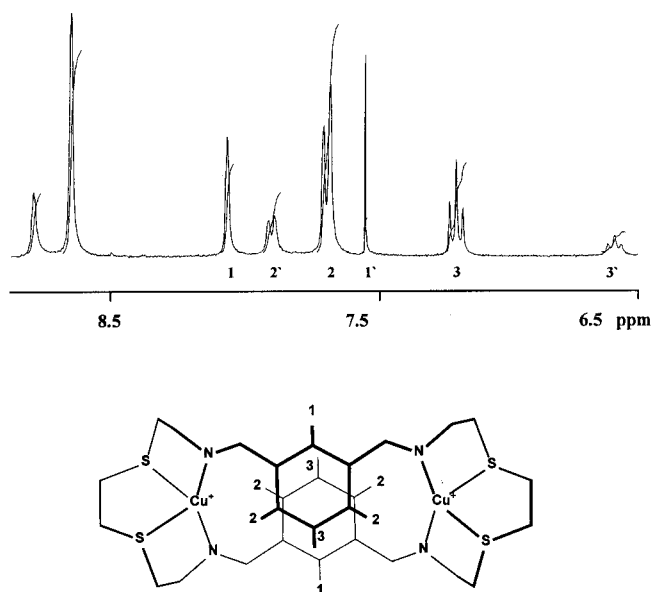


Figure 2. Region of the signals of the aromatic protons in the ^1H -NMR spectrum (200 MHz, 290 K, CD_3NO_2) of $[\text{Cu}_2(\text{meta-222})]^{2+}$; the numbering of the protons of the *meta*-xylylene groups is given in the sketch

tons: < 230 K, solvent-independent; methylene protons (only in acetonitrile): 300 K}. This suggests that intramolecular processes for $[\text{Cu}_2(\text{meta-222})]^{2+}$ have significantly higher activation barriers. Based on the structural features of the “squeezed” geometry this is not unexpected: The stack-and-slip process (Scheme 1) must lead to a significant amount of unfolding and strain in the copper(I)–donor bonds, especially for the experimentally observed tail-to-tail rotamer; the reorientation of the *meta*-xylylene spacer groups (tail-to-tail/head-to-tail/head-to-head isomerization) involves a rotation around the $\text{C1}\cdots\text{C3}$ axis, and this is sterically less favorable than the corresponding rotation of the *para*-xylylene spacer groups ($\text{C1}\cdots\text{C4}$ axis). The fact that the high-temperature dynamic process is only moderately dependent on the solvent for $[\text{Cu}_2(\text{meta-222})]^{2+}$ suggests that $\text{Cu}^{\text{I}}\text{—S}$ bond breaking has a more dissociative activation than for $[\text{Cu}_2(\text{para-222})]^{2+}$, and this is supported by the higher activation barrier of the low-temperature dynamics, that is, these processes involve highly strained transition states. Further support for this interpretation emerges from the observation that the air stability of the $[\text{Cu}_2(\text{meta-222})]^{2+}$ species is considerably lower than that of $[\text{Cu}_2(\text{para-222})]^{2+}$, that is, oxygenation of the dicopper(I) compound is probably also activated along the intramolecular dynamic process.

In the region of the aromatic and imine proton signals one expects a singlet for the imine protons and three signals for the aromatic protons (singlet, doublet, triplet) in the ratio 2:1:2:1. The experimental ^1H -NMR spectrum at 298 K (Figure 2) suggests that two isomeric $[\text{Cu}_2(\text{meta-222})]^{2+}$ species in the ratio of approximately 3:1 are present in solution. There is only one set of signals in the region of aliphatic protons, suggesting that the coordination geometries

of the two isomers are close to identical [the sum of the integrals of the signals in the aromatic region (both isomers) corresponds to that expected from the sum of integrals of the aliphatic protons]. Possible isomeric forms [tail-to-tail (observed in the solid state, see Figure 1), head-to-tail, head-to-head] are shown in Scheme 3. The experimental spectrum suggests that only two species are stable in solution. Also, the head-to-tail isomer has a lower symmetry, and additional splitting in the aromatic region would be expected for this species, unless a fast dynamic exchange occurred.

Further structural information emerges from a qualitative analysis of the chemical shifts in the aromatic region (Table 2; see structural sketch in Figure 2 for proton numbering). Based on the solid-state structure (Figure 1; the *meta*-xylylene rings are stacked with a xylylene \cdots xylylene distance of 3.39 Å and a horizontal displacement of the two rings by 1.06 Å^[3]) one expects that signals of protons 2 and especially 3 are shifted to higher field due to dipole-dipole interactions with the other aromatic ring, while there is less interaction with protons 1. The observed signals of the major species are in agreement with these expectations (shift with respect to the chemical shift of the metal-free ligand of $\Delta\delta = +0.07, -0.11, -0.31$ for signals 1, 2, 3, respectively). In the less abundant isomer (primed resonances in Figure 2), the signals for proton 1' and 3' are shifted to higher field with respect to those in the major isomer ($\Delta\delta = -0.53$ and -1.52), indicating that there is a very strong interaction with the other aromatic ring. For protons 2' there is a decreasing interaction ($\Delta\delta = +0.21$). This behavior may be interpreted by a tilt of the two aromatic planes with respect to each other (see rotation of the xylylene rings above). The relative symmetry (number of symmetry-related protons) suggests that a fast equilibrium between various sites must be involved, that is, in average, both *meta*-xylylene rings are equivalent.

Modeling Studies

Empirical force-field calculations in combination with experimental data (isomer distributions, reduction potentials, EPR, NMR and electronic spectra) have been used extensively to determine structures of transition metal compounds in solution.^[8–11] The MOME program^[12] and force field^[13] have been tested successfully in this field, and in various areas they have demonstrated to lead also to accurate predictions of conformational equilibria and energy barriers for conformer interconversions.^[14] This is not necessarily expected since the force field is primarily based on solid-state structural data.^[14] However, the parameter sets used for the ligand backbones are transferable, and from the fact that some of these parameters were fitted to thermodynamic observables it emerges that the steepnesses of the potentials are approximately realistic. Published studies, primarily in the fields of (hexamine)cobalt(III) and -nickel(II) compounds support this suggestion.^[8–11,14] The new parameters necessary to model the conformational

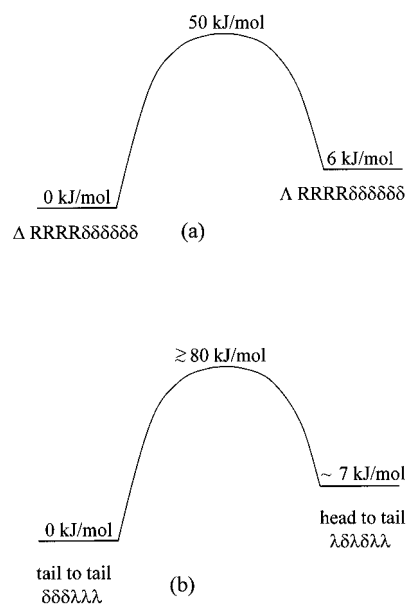
Table 2. $^1\text{H-NMR}$ data of meta-222 and $[\text{Cu}_2(\text{meta-222})]^{2+}$ [200 MHz, CD_3NO_2 , 290 K (and 350 K), low-field region, δ (ppm)]; for atom numbering, see Figure 2

	Metal-free ligand 290 K	Major isomer 290 K	Minor isomer 290 K	Fast exchange 350 K
imine proton	8.3	8.68	8.82	8.70
aromatic proton 1	8.0	8.07	7.54	8.01
aromatic proton 2	7.8	7.69	7.90	7.75
aromatic proton 3	7.5	7.19	5.57	7.05

space of $[\text{Cu}_2(\text{para-222})]^{2+}$ and $[\text{Cu}_2(\text{meta-222})]^{2+}$ include copper(I)–thioether–S interactions and a few parameters involving the substituents of the thioether and Schiff base donors (see Experimental Section). These were fitted to the published experimental structures in this series.^[1–4] Thus, the expectation was that, together with the experimental data discussed above, a full conformational analysis of the two isomers $[\text{Cu}_2(\text{para-222})]^{2+}$ and $[\text{Cu}_2(\text{meta-222})]^{2+}$ would lead to some insight into the dynamic processes in these systems.

$[\text{Cu}_2(\text{para-222})]^{2+}$

The conformation observed in the solid $\{\Lambda\text{-(S)(S)(S)(S)-}\lambda\lambda\lambda\lambda\lambda\lambda\text{-}[\text{Cu}_2(\text{para-222})]^{2+}\}$ is the most stable structure ($U_{\text{strain}} = 28 \text{ kJ/mol}$). Inversion of a five-membered chelate ring costs approximately 5 kJ/mol and inversion of a coordinated thioether–S center leads to a destabilization of approximately 16 kJ/mol. These effects are not additive but the next lowest energy structure (five-membered ring inversions alone excluded; these have activation barriers of approximately 25 kJ/mol,^[15,16] i.e. their interconversion will not be frozen at the low-temperature limits of our experimental studies) is that of the helix inversion product, i.e. $\Delta\text{-(S)(S)(S)(S)-}\lambda\lambda\lambda\lambda\lambda\lambda\text{-}[\text{Cu}_2(\text{para-222})]^{2+}$ with $U_{\text{strain}} = 34 \text{ kJ/mol}$. The strain energy minimization of structures with constrained pseudo-torsional angles ϕ around the centroids of the two *para*-xylylene rings (helix inversion; $\phi = 80^\circ$ to $\phi = -80^\circ$) was not as straightforward as one might anticipate. Without any further constraints there was a considerable distortion in the stacking of the *para*-xylylene rings that lead to intermediate structures at the transition state (pseudo-torsional angle $\phi = 0^\circ$) with horizontal translations or tilts of the two *para*-xylylene rings. This supports the interpretation based on the solution $^1\text{H-NMR}$ studies that, along the helix inversion, there is a low-energy rotation of the *para*-xylylene rings (see above). Also, with constrained stacking, the distance between the *para*-xylylene rings increases at the transition state ($\phi = 0^\circ$) from approximately 3.3 Å to approximately 4.9 Å. The energy barrier of the helix inversion process with constrained stacking of the *para*-xylylene rings is approximately 50 kJ/mol (see Figure 3). This upper limit of the activation energy for the helix inversion process is in good qualitative agreement with the temperature-dependent $^1\text{H-NMR}$ data.^[4]

Figure 3. Energy profile of the dynamic processes of (a) $[\text{Cu}_2(\text{meta-222})]^{2+}$ and (b) $[\text{Cu}_2(\text{para-222})]^{2+}$

$[\text{Cu}_2(\text{meta-222})]^{2+}$

Only two of the three putative rotamers of $[\text{Cu}_2(\text{meta-222})]^{2+}$ (Scheme 3) converged to a stable structure. The experimentally observed geometry $\{\text{tail-to-tail-(R)(R)(S)(S)-}\delta\delta\delta\lambda\lambda\lambda\text{-}[\text{Cu}_2(\text{meta-222})]^{2+}\}$ was that with the lowest strain energy ($U_{\text{strain}} = 40 \text{ kJ/mol}$; that is, the isomer with *meta*-xylylene spacer groups is approximately 12 kJ/mol less stable than that with *para*-xylylene spacer groups). The energy differences to species with inverted five-membered chelate rings and inverted thioether–S donor groups are similar to those of the *para* isomer (see above). Optimization of the head-to-tail isomer leads to a structure with one of the two aromatic rings tilted with respect to the other (see Figure 4). Optimization of the third rotamer (head-to-head) converged to either of the two other structures (head-to-tail or tail-to-tail), that is, this is not a minimum on the energy surface. The most stable head-to-tail conformer is head-to-tail-(R)(R)(S)(S)- $\lambda\delta\lambda\delta\lambda\lambda\text{-}[\text{Cu}_2(\text{meta-222})]^{2+}$ with $U_{\text{strain}} = 47 \text{ kJ/mol}$.^[17] The strain energy difference between the two rotamers (7 kJ/mol) is in good agreement with the isomer distribution observed in the $^1\text{H-NMR}$ spectrum (3:1, Figure 2). The optimized structure of the less abundant head-to-tail isomer is of particular interest since it is as expected

from the solution $^1\text{H-NMR}$ spectroscopic data, that is, the two aromatic spacer groups are tilted with respect to each other (see above). The sketches shown in Scheme 3 indicate that this might be due to the relieve of some strain related to the geometry around the C-1 and C-3 bridgehead carbon atoms of the *meta*-xylylene spacer group.

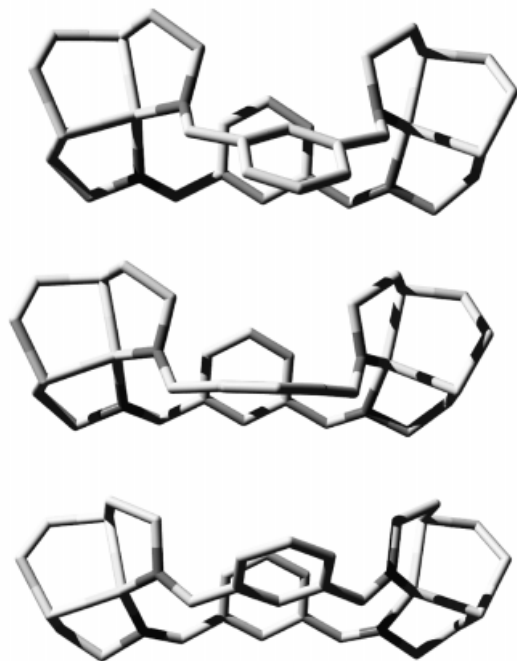


Figure 4. Visualization of the low-temperature dynamic process of the head-to-tail isomer of $[\text{Cu}_2(\text{meta-222})]^{2+}$

Constraints were used to map the interconversion of the two rotamers of $[\text{Cu}_2(\text{meta-222})]^{2+}$. The qualitative picture (see Figure 3) is that there is an activation energy between the two isomers of at least 80 kJ/mol. This is consistent with the observation that, at low temperature ($< 300\text{ K}$) there is no fast interconversion of the two isomers. Especially interesting is the observation that, for the tilted head-to-tail isomer there is a very shallow energy surface with at least three minima where the tilt angle between the two xylylene planes varies from approximately 30° to approximately 120° (see Figure 4). In the enforced structure of the head-to-tail isomer with parallel aromatic rings (transition state) the two *meta*-xylylene rings are symmetry-related, that is, there is a wagging mode of the two rings with an energy barrier of less than approximately 25 kJ/mol, and this is consistent with the observed $^1\text{H-NMR}$ spectra (see above). That is, the observed chemical shifts are due to the tilt of one of the xylylene planes with respect to the other and the shallow energy minima with various structural modes is in agreement with the observed high symmetry averaged structure.

Experimental Section

The syntheses have been described before.^[1–4] – NMR spectra were obtained with a Bruker AS200 instrument at 200 MHz. – MOMECC97^[12,13] with a published force field^[12] was used to com-

pute the optimized structures and minimized strain energies. Parameters not published before are given in Table 3.

Table 3. MOMECC force-field parameters^[a]

		Bond lengths			
Type 1	Type 2	k [mdyn \AA^{-1}]	r_0 [\AA]		
N_{imine}	C_{methyl}	3.4	1.48		
Cu^{I}	$\text{S}_{\text{thioether}}$	0.1	2.30		
$\text{C}_{\text{benzene}}$	O_{ether}	5.0	1.36		
$\text{C}_{\text{benzene}}$	$\text{S}_{\text{thioether}}$	4.0	1.42		
$\text{C}_{\text{benzene}}$	N_{imine}	4.0	1.42		
		Torsion angles			
Type 1	Type 2	k [mdyn \AA]	m	ϕ_0 [rad]	
C_{imine}	$\text{C}_{\text{benzene}}$	0.005 (0.025) ^[b]	2	1.571	
$\text{C}_{\text{benzene}}$	$\text{C}_{\text{benzene}}$	0.060	2	1.571	
		Valence angles			
Type 1	Type 2	Type 3	k [mdyn $\text{\AA} \text{ rad}^{-2}$]	θ_0 [rad]	
$\text{S}_{\text{thioether}}$	Cu(I)	N_{amine}	0	0	
N_{imine}	Cu(I)	N_{imine}	0	0	
Cu^{I}	$\text{S}_{\text{thioether}}$	C_{methyl}	0.10	1.745	
Cu^{I}	$\text{S}_{\text{thioether}}$	$\text{C}_{\text{benzene}}$	0.10	1.571	
Cu^{I}	N_{imine}	$\text{C}_{\text{benzene}}$	0.10	2.094	
$\text{C}_{\text{benzene}}$	$\text{S}_{\text{thioether}}$	C_{methyl}	0.50	1.740	
$\text{C}_{\text{benzene}}$	$\text{C}_{\text{benzene}}$	$\text{S}_{\text{thioether}}$	0.45	2.094	
$\text{C}_{\text{benzene}}$	N_{imine}	C_{imine}	0.50	2.094	
$\text{C}_{\text{benzene}}$	$\text{C}_{\text{benzene}}$	N_{imine}	0.50	2.094	
$\text{C}_{\text{benzene}}$	O_{ether}	C_{methyl}	0.75	2.094	
$\text{C}_{\text{benzene}}$	$\text{C}_{\text{benzene}}$	O_{ether}	0.75	2.094	
O_{ether}	C_{methyl}	H	0.36	1.911	
C_{methyl}	$\text{O}_{\text{alcohol}}$	H	0.35	1.870	

^[a] All other parameters have been published before.^[13] – ^[b] See ref.^[17]

Acknowledgments

Generous financial support by the German Science Foundation (DFG) and the Fund of the Chemical Industry (FCI) are gratefully acknowledged.

- [1] P. Comba, A. Fath, G. Huttner, L. Zsolnai, *Chem. Commun.* **1996**, 1885.
- [2] P. Comba, A. Fath, T. W. Hambley, D. T. Richens, *Angew. Chem. Int. Ed. Engl.* **1995**, 34, 1883.
- [3] P. Comba, A. Fath, T. W. Hambley, A. Vielfort, *J. Chem. Soc., Dalton Trans.* **1997**, 1691.
- [4] P. Comba, A. Fath, T. W. Hambley, A. Kühner, D. T. Richens, A. Vielfort, *Inorg. Chem.* **1998**, 37, 4389.
- [5] D. J. Cram, T. Kamda, R. L. Helgeson, G. M. Liu, *J. Am. Chem. Soc.* **1979**, 99, 948.
- [6] D. J. Cram, G. M. Liu, *J. Am. Chem. Soc.* **1985**, 107, 3657.
- [7] P. Comba, *Coord. Chem. Rev.*, in press.
- [8] P. Comba, in *Fundamental principles of molecular modeling* (Eds.: W. Gans, A. Amann, J. C. A. Boeyens), Plenum Press, New York, **1996**, p 167.
- [9] P. Comba, in *Molecular modeling and dynamics of bioinorganic systems* (Eds.: L. Banci, P. Comba), Kluwer Dordrecht, Boston, **1997**, p 21.
- [10] P. Comba, in *Intermolecular Interactions* (Eds.: W. Gans, J. C. A. Boeyens), Plenum Press, New York, **1998**, p 97.
- [11] P. Comba, in *Implications of Molecular and Materials Structure for New Technologies* (Eds.: J. K. A. Howard, F. H. Allen), Kluwer, Dordrecht, **1998**.

- [12] P. Comba, T. W. Hambley, N. Okon, G. Lauer, *MOMEC, a molecular modeling package for inorganic compounds*, CVS, E-mail: cvs@t-online.de, Heidelberg, **1997**.
- [13] J. E. Bol, C. Buning, P. Comba, J. Reedijk, M. Ströhle, *J. Comput. Chem.* **1998**, *19*, 512.
- [14] P. Comba, T. W. Hambley, *Molecular Modeling of Inorganic Compounds*, VCH, Weinheim, **1995**.
- [15] T. W. Hambley, *J. Comput. Chem.* **1987**, *8*, 651.
- [16] Y. Kuroda, N. Tanaka, M. Goto, T. Sakai, *Inorg. Chem.* **1989**, *28*, 997.
- [17] Detailed studies that involved the reported structures and isomer distributions of all figure-of-eight-shaped dicopper(I) com-

pounds indicate that some of the force-field parameters need some further tuning. One of the critical parameters was the torsional angle force constant for the C_{xylylene}–C_{imine} bond. The steepness of this potential is probably overestimated, and an optimum fit was obtained when this parameter was reduced from $k = 0.025 \text{ m dyn} \cdot \text{Å}$ by a factor of up to 5. This observation is based on the very restricted class of compounds discussed here, and future studies with other types of compounds are needed to establish this parameter on a more general basis.

Received September 29, 1998
[I98334]